JOURNAL OF AIRCRAFT
Vol. 43, No. 5, September–October 2006

Robust Objective Functions for Sonic-Boom Minimization

Yoshikazu Makino*
Japan Aerospace Exploration Agency, Tokyo 181-0015, Japan
and
Ilan Kroo†
Stanford University, Stanford, California 94305

DOI: 10.2514/1.19442

Some metrics for sonic-boom intensity used as an objective function are studied for robust sonic-boom minimization. Conventional sonic-boom metrics such as initial and final pressure rises or the A-weighted decibel evaluation may introduce unrealistic low sonic-boom pressure signatures which include some sets of consecutive shock pressure peaks at a very short interval. Some new metrics, the A-weighted decibel with a penalty for very short pressure peak intervals or sonic-boom signature mold line evaluations, are shown to be useful to avoid such unrealistic signatures. Minimizing sonic boom across the boom carpet instead of just under the flight path is important for more robust sonic-boom minimization.

Nomenclature

C_L	=	lift coefficient
C_p	=	pressure coefficient
$F(x)$	=	Whitham's F function
H	=	vertical downward distance from airplane
I	=	objective function to be minimized through optimization process
L	=	airplane length
M	=	flight Mach number
x	=	axial coordinate of airplane
Y	=	lateral distance from flight path
β	=	$\sqrt{M^2-1}$
γ	=	specific heat ratio
Δp	=	pressure difference from ground ambient pressure
ΔT	=	time interval between two consecutive pressure peaks in signature
Δx	=	nonlinear deformation of pressure signature
τ	=	rise time of pressure jump in signature

Subscripts

final	=	final pressure rise in signature
initial	=	initial pressure rise in signature
max	=	maximum pressure rise in signature
SML	=	signature mold line

I. Introduction

SONIC boom is one of the biggest environmental problems for supersonic transport (SST) since the development of first generation SST like the Concorde in the 1960s. Some low sonic-boom pressure signatures which are quieter than the usual N-shaped sonic-boom signature have been proposed to reduce sonic boom. In the Quiet Supersonic Platform (QSP) program [1] sponsored by the Defense Advanced Research Projects Agency (DARPA), flight tests of the Shaped Sonic Boom Demonstrator (SSBD), which was designed to generate one of the low-boom signatures by modifying the nose configuration of an F-5 airplane, were successfully conducted and flat-top type low-boom signatures were measured on the ground [2]. In the conventional low-boom designs like the SSBD, some kinds of inverse methods [3] based on linear theory for an axisymmetrical body are used to generate low-boom signatures. Recently direct optimization of an airplane configuration to reduce its sonic-boom intensity was studied. Chan [4] developed the low-drag and low-boom design tool using the multiobjective genetic algorithm (GA) in which both the drag and the sonic boom of an airplane are minimized. In such a direct sonic-boom minimization, the definition of sonic-boom intensity as an objective function is important because some objective functions sometimes introduce "sensitive" low-boom signatures which include some sets of consecutive pressure peaks at a very short interval and can easily become noisy sonic-boom signatures by small changes in the flight or atmospheric conditions.

In this study, the problems of the sensitive low-boom signatures for conventional sonic-boom metrics as an objective function in direct sonic-boom minimization are described and some new metrics are proposed for a robust sonic-boom minimization.

II. Airplane Configuration

The airplane characteristics of a supersonic business jet (SSBJ) configuration used in this study are shown in Table 1. Figure 1 shows one example of the SSBJ configurations with a low-drag designed fuselage. The main wing plan form is fixed in this study and the NACA64-003 is used as its airfoil. For stable flow simulations by a panel method, the engine nacelle of the airplane is simulated by an axisymmetrical body whose cross section area is equal to that of a flow-through nacelle configuration. A T-tail type stabilizer is considered, however, its vertical tail is omitted for simplicity because it does not seem to have a strong impact on near-field pressure signatures below the airplane. Twelve design variables used in the low-boom design are shown in Table 2. Axisymmetrical fuselage radii are defined at $x/L = 0.05, 0.1, 0.2, 0.3, 0.5, 0.6$, and 0.8 by the design variables dv1–7, respectively. The fuselage shape is determined by these radii using an Akima spline [5]. The minimum radius constraints of 2.5 and 3.1 ft are specified at $x/L = 0.2$ and 0.3, respectively, for crew and cabin space. The ranges of the design variables are specified so that they can represent both low-drag and low-boom configurations while they are kept as small as possible for fast design convergence. The micro-GA [6] optimizer which is suitable for multimodal objective functions is used in the sonic-boom minimization.

Received 11 August 2005; revision received 12 December 2005; accepted for publication 16 January 2006.

*Senior Researcher, SST Team, Aviation Program Group, 6-13-1 Osawa, Mitaka. AIAA Member.
†Professor, Department of Aero/Astro, AIAA Fellow.

Table 1 Airplane characteristics

Flight Mach number	1.5
Flight altitude	50,000 ft
Airplane weight	70,000 lb
Fuselage length	108 ft
Wing span	64.8 ft
Wing area	1650 ft^2
Wing aspect ratio	2.545

Table 2 Design variables

dv1	Fuselage radius at $x/L = 0.05$ (0.8–2 ft)
dv2	Fuselage radius at $x/L = 0.1$ (dv1 < dv2 < dv1 + 0.8 ft)
dv3	Fuselage radius at $x/L = 0.2$ (2.5–2.6 ft)
dv4	Fuselage radius at $x/L = 0.3$ (3.1–3.2 ft)
dv5	Fuselage radius at $x/L = 0.5$ (2.5–3.0 ft)
dv6	Fuselage radius at $x/L = 0.6$ (2.0– 2.5 ft)
dv7	Fuselage radius at $x/L = 0.8$ (1.5–1.8 ft)
dv8	Wing root incidence (0.5–1 deg)
dv9	Wing twist at break point (−2–−1.5 deg)
dv10	Wing twist at tip (−3–−2.5 deg)
dv11	Horizontal tail x location (105–108 ft)
dv12	Horizontal tail root incidence (−1–−0.5 deg)

III. Sonic-Boom Analysis

The ground sonic-boom signatures of the SSBJ configurations are predicted by the A502 panel method [7] and the Thomas sonic-boom propagation method [8]. The A502, also known as Panair, is a computer program to solve the aerodynamic properties for arbitrary aircraft configurations at subsonic and supersonic speeds. The program uses a higher-order (quadratic doublet, linear source) three dimensional panel method, based on the solution of the linearized potential flow boundary-value problem. Figure 1 shows the surface C_p distribution of a low-drag configuration calculated by the A502. This calculation used 440 panels for the main wing, 390 panels for the fuselage, 56 panels for the horizontal tail, and 49 panels for simulated nacelle. Near-field pressure distributions are also calculated in the A502 analysis and used as input data for ground sonic-boom signatures prediction. Figure 2 shows some near-field pressure signatures of the low-drag configuration at two airplane lengths below the airplane ($H/L = 2.0$) predicted by the A502. This position of input near-field pressure signature where quasiacoustic propagation can be applied is determined for this airplane configuration after checking the ground signature convergence. The near-field pressure signatures on several lines under the airplane as shown in Fig. 2 are needed to predict the sonic boom across the boom carpet. Near-field aging effects which mean the nonlinear distortion of the signatures are considered in the same way as described in [4]. Figure 3 which is reproduced from [4] shows that the output signature from the A502 with this near-field aging correction agrees well with the result of an Euler CFD analysis (shown as QSP107 in the figure). Whitham's F function [9] is calculated from the predicted near-field pressure signature using Eq. (1) and the distortion of the signature is calculated using Eq. (2) from the F function:

$$F(x) = \sqrt{\frac{\beta r}{2}} C_p \tag{1}$$

$$\Delta x = -\frac{(\gamma+1)}{\sqrt{2\beta^3}} \sqrt{r} F(x) \tag{2}$$

When the signature has multiple pressure values at some x locations by distorting it with Eq. (2), the area-balancing technique is used to define shock waves in the signature. The signatures shown in Fig. 2 are those after the near-field aging corrections. The Thomas method, also known as the waveform parameter method, is a computer program based on a modified linear theory to extrapolate near-field pressure signatures measured in wind-tunnel tests or predicted by numerical analyses to the ground. This method considers the nonlinear distortion of pressure signatures and the altitudinal distribution of atmospheric properties such as temperature and wind. The rise time of a pressure jump which is important in the A-weighted decibel (dBA) evaluation of a ground pressure signature is not predicted in the Thomas method and the output ground pressure signature includes some discontinuous ($\tau = 0$) pressure jumps. In this study, the rise time for each pressure jump is estimated by an empirical

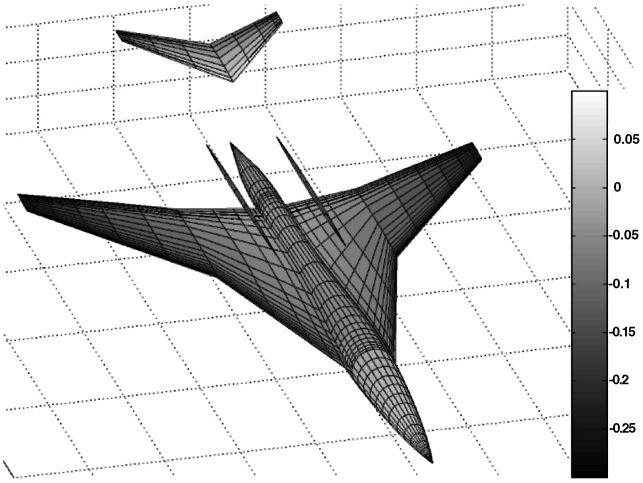

Fig. 1 Low-drag configuration (surface C_p).

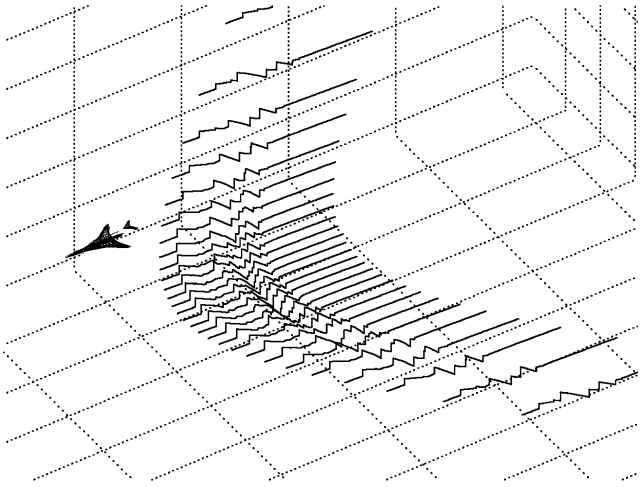

Fig. 2 Near-field pressure signatures ($H/L = 2.0$).

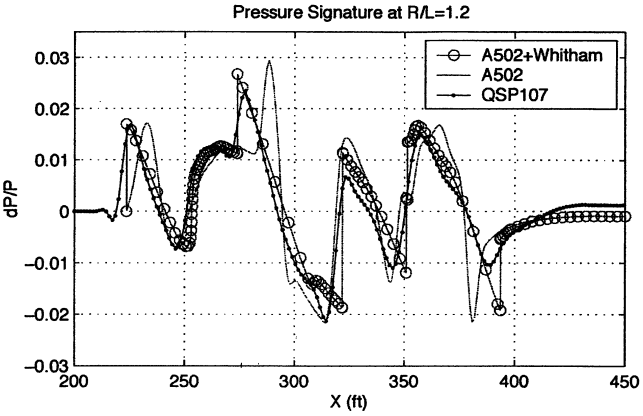

Fig. 3 Near-field aging effect ([4]).

model [10] as follows:

$$\tau[\text{sec}] = \frac{0.003}{\Delta p[\text{psf}]} \tag{3}$$

The rise time upper bound of $\tau < 3$ ms is used to avoid an unrealistic long rise time for a very small pressure rise.

IV. Sensitive Signature Problems in Sonic-Boom Minimization with Conventional Sonic-Boom Metrics

A. Initial and Final Pressure Rises

Figure 4 shows one example of the sensitive low-boom signatures that is obtained in the sonic-boom minimization using the following objective function:

$$I = \Delta p_{\text{initial}} + \Delta p_{\text{final}} \tag{4}$$

In this design example, the objective function is evaluated only just under the flight path where the sonic-boom intensity is thought to be strongest. Figure 4 shows the optimized low-boom signature on the ground just under the flight path ($Y = 0$ mile). Upon first viewing this figure, the initial pressure rise seems to be $\Delta p = 0.3$ psf, but this pressure rise comprises two pressure rises shown in the close-up figure. A second pressure rise of $\Delta p = 0.25$ psf follows the first very small pressure rise of $\Delta p = 0.05$ psf at a very short interval of $\Delta T = 0.01$ ms. These consecutive pressure peaks at a very short interval should be regarded as one pressure rise of $\Delta p = 0.3$ psf because the human ear cannot distinct such a short time difference and moreover this signature seems to be very sensitive to any changes in flight or atmospheric conditions.

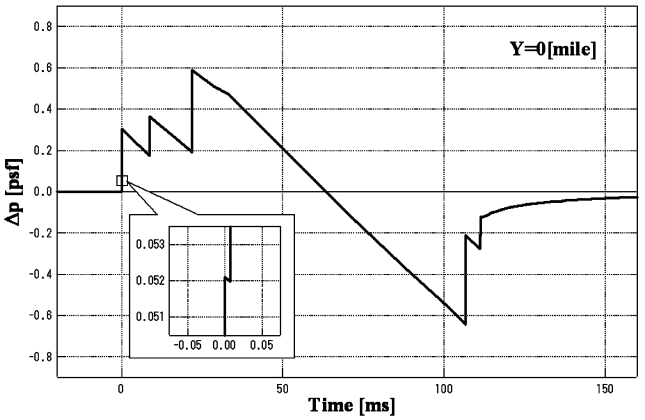

Fig. 4 Sonic-boom minimization for initial and final pressure rise.

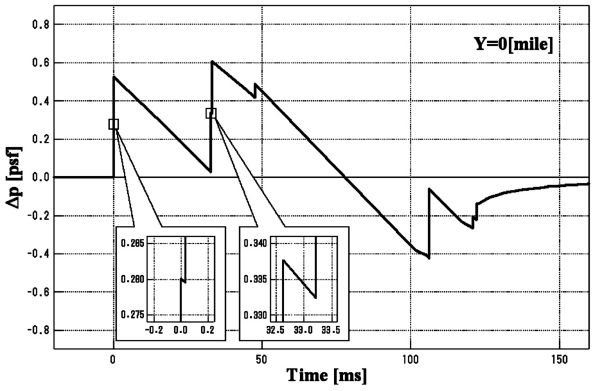

a) Optimized sonic-boom signature at Y=0mile.

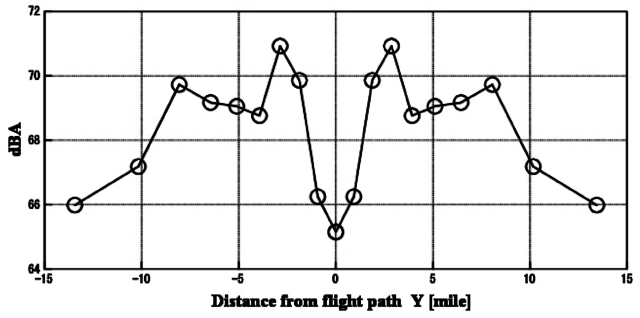

b) dBA distribution across the boom carpet.

Fig. 5 Sonic-boom minimization for dBA.

B. dBA

Figure 5 shows another sonic-boom minimization example in which the dBA value of a sonic-boom signature predicted just under the flight path is used as an objective function. In [11], the dBA evaluations of sonic-boom signatures are shown to have a good

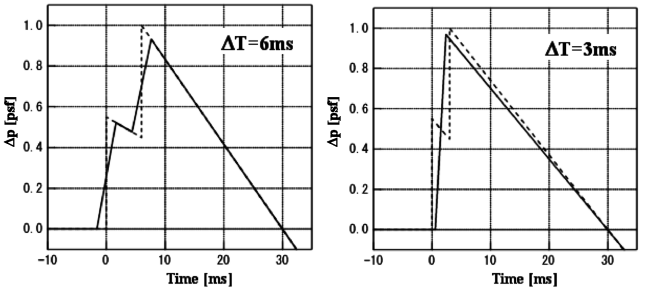

Fig. 6 Signature modification for sensitive signature penalty.

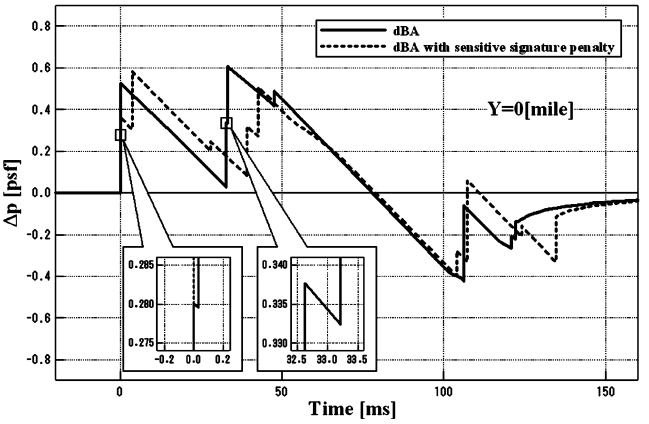

Fig. 7 Sonic-boom minimization for dBA with sensitive signature penalty.

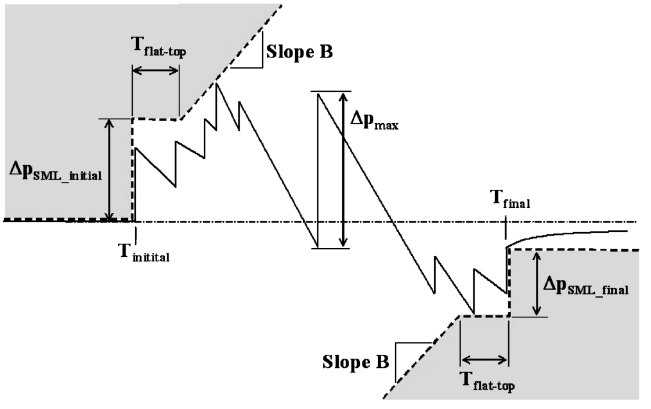

Fig. 8 Signature mold line definition.

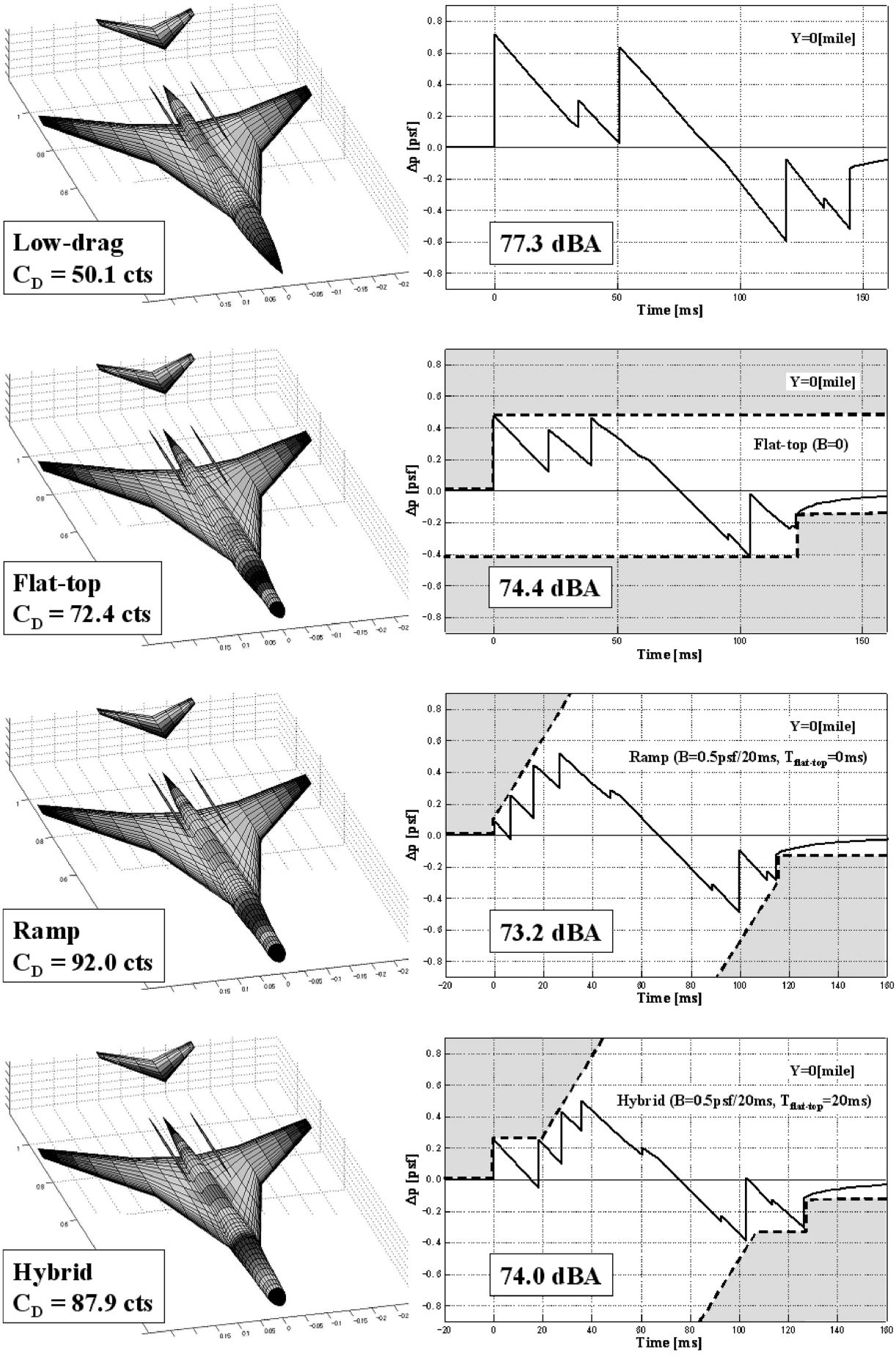

Fig. 9 Sonic-boom minimization using signature mold line evaluation.

correlation with human responses as well as the Stevens perceived noise level (PLdB) [12]. The optimized low-boom signature under the flight path shown in Fig. 5a is a sensitive signature similar to the previous design case. The first pressure rise of 0.53 psf comprises two pressure rises of 0.28 and 0.25 psf at an interval of 0.03 ms. The pressure rise around $T = 40$ ms also comprises two pressure rises of 0.3 and 0.27 psf at an interval of 0.6 ms. This design result suggests that the sonic-boom minimization for dBA tends to divide a large pressure peak into several small pressure peaks at short intervals. Figure 5b shows the sonic-boom loudness distribution across the boom carpet. It shows that the dBA value is minimized only just under the flight path, and it increases about 6 dBA about 3 miles aside of the flight path because the short intervals as shown in Fig. 4 disappear and some large pressure rises are formed in the signature.

Two handlings are needed to avoid these sensitive signatures shown in the previous design examples. One handling is to use the maximum sonic-boom intensity across the boom carpet as an objective function. But still the sensitive signature may appear somewhere in the boom carpet. Another handling is to use a certain robust sonic-boom metric as an objective function, which cannot accept any sensitive signatures. Such robust sonic-boom metrics are described in the next section.

V. New Sonic-Boom Metrics for Robust Sonic-Boom Minimization

A. dBA with Sensitive Signature Penalty

One simple way to avoid the sensitive signatures is to use the dBA value with a certain penalty for a very short interval between two consecutive pressure peaks. In this study, such a penalty is considered by modifying a signature before the dBA evaluation. A sonic-boom signature predicted by the Thomas method is modified with the estimated rise time as shown in the left figure of Fig. 6. When the interval of two consecutive pressure peaks in the signature is shorter than the average rise time for the peaks, they are regarded as one pressure peak and are modified as shown in the right figure of Fig. 6. The result of the sonic-boom minimization just under the flight path using this dBA evaluation with the penalty effects is shown in Fig. 7. Compared to the case of using the normal dBA, the optimized signature with this dBA evaluation shows robustness for the sensitive signature. Because this signature modification like shock merging is very simplified, the dBA value itself should not be used for human acceptability study. The other modification based on physical shock thickening mechanisms such as a molecular relaxation absorption theory should be used for such a purpose.

B. Signature Mold Line Evaluation

In [4], Chan suggested that minimizing the difference between the maximum and the minimum pressure in a signature is more robust metric than the normal dBA. This evaluation is equivalent to minimize the distance between the imaginary walls above and below the sonic-boom signature and a flat-top type low-boom signature is one of the optimized signatures for this metric. A signature mold line evaluation proposed in this section as another robust sonic-boom metric is an extended version of this metric by changing the wall shapes to represent the other types of low-boom signatures. Compared to the dBA with the sensitive signature penalty, the signature mold line evaluation has an advantage of specifying a target low-boom signature. The signature mold line shown by the dashed line in Fig. 8 is defined by two parameters specified by a designer. Slope B is used to represent the ramp and hybrid-type low-boom signatures and $T_{\text{flat top}}$ is used for the hybrid-type low-boom signature. Although this signature mold line method is robust at the initial and final parts of a signature, the maximum pressure rise in the signature may increase the dBA value of the signature if it is larger than $\Delta p_{\text{SML}_{\text{initial}}}$ and $\Delta p_{\text{SML}_{\text{final}}}$. Therefore the following objective function is used in the signature mold line evaluation.

$$I = \Delta p_{\text{SML}_{\text{initial}}} + \Delta p_{\text{SML}_{\text{final}}} + \max(0, \Delta p_{\max} - \Delta p_{\text{SML}_{\text{initial}}}, \Delta p_{\max} - \Delta p_{\text{SML}_{\text{final}}}) \quad (5)$$

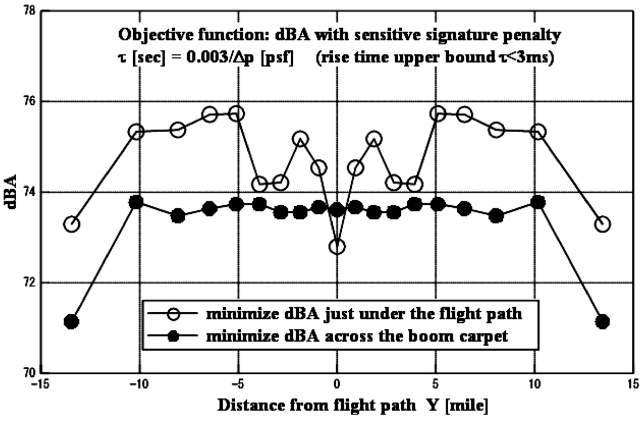

Fig. 10 Sonic-boom minimization across the boom carpet.

Additionally, the signature modification described in the previous section is used to avoid sensitive signatures around the maximum pressure rise. Because this objective function tends to reduce the maximum pressure rise in the signature, it seems to reduce the dBA value of the signature. The detail of the correlation between this signature mold line metric and the sonic-boom impact should be studied in future work. The results of sonic-boom minimization using this objective function evaluated just under the flight path are shown in Fig. 9. The target three types of low-boom signatures, flat-top type ($B = 0$, $T_{\text{flat top}} = 0$ ms), ramp type ($B = 0.5$ psf/20 ms, $T_{\text{flat top}} = 0$ ms), and hybrid type ($B = 0.5$ psf/20 ms, $T_{\text{flat top}} = 20$ ms) are successfully generated on the ground by this objective function. In the figure, each airplane configuration is shown with its airplane drag in drag counts (1 drag count = 0.0001) at cruise C_L.

VI. Sonic-Boom Minimization Across the Boom Carpet

As previously suggested, the sonic boom should be minimized across the boom carpet for robust low-boom design even if the previous robust metrics are used as objective functions. Figure 10 compares the low-boom design result across the boom carpet with the one minimized just under the flight path. The lateral distribution of dBA minimized across the boom carpet becomes flat whereas the dBA distribution obtained by the low-boom design just under the flight path has a smaller dBA value only at the center line ($Y = 0$ mile).

VII. Conclusion

Some new sonic-boom metrics are studied to avoid sensitive low-boom signatures obtained in sonic-boom minimization using conventional sonic-boom metrics. The low-boom design examples show that the sensitive signature penalty makes the dBA evaluation robust. The signature mold line evaluation in which a designer can specify a target low-boom signature is also a robust metric and three types of low-boom signatures are successfully obtained in the low-boom design of an SSBJ configuration. The sonic-boom minimization across the boom carpet instead of just under the flight path is important for robust low-boom design. Although the sonic-boom metrics proposed here showed the importance of analytical robustness of the objective functions in sonic-boom minimization, they do not necessarily guarantee the minimum boom impact. Further studies of correlation between the metrics and the sonic-boom impact are needed.

References

[1] Wlezien. R., and Veitch. L., "Quiet Supersonic Platform Program," AIAA Paper 2002-0143, Jan. 2002.

[2] Plotkin, K. J., Haering, E. A., Jr., Murray, J. E., Maglieri, D. J., Salamone, J., Sullivan, B. M., and Schein, D., "Ground Data Collection of Shaped Sonic Boom Experiment Aircraft Pressure Signatures,"

AIAA Paper 2005-010, Jan. 2005.
[3] Darden, C. M., "Sonic-Boom Minimization with Nose-Bluntness Relaxation," NASA TP-1348, Jan. 1979.
[4] Chan, M. K., "Supersonic Aircraft Optimization for Minimizing Drag and Sonic Boom," Ph.D. Dissertation, Stanford University, Aug. 2003.
[5] Akima, H., "A Method of Univariate Interpolation that has the Accuracy of a Third Degree of Polynomial," *ACM Transaction on Mathematical Software*, Vol. 17, No. 3, Sept. 1991, pp. 341–366.
[6] Carroll, D. L., "Chemical Laser Modeling with Genetic Algorithms," *AIAA Journal*, Vol. 34, No. 2, Feb. 1996, pp. 338–346.
[7] Carmichael, R. I., and Erickson, L. I., "PANAIR—A Higher Order Panel Method for Predicting Subsonic or Supersonic Linear Potential Flows about Arbitrary Configurations," AIAA Paper 81-1255, June 1981.
[8] Thomas, C. L., "Extrapolation of Sonic Boom Pressure Signatures by the Waveform Parameter Method," NASA TN D-6832, June 1972.
[9] Whitham, G. B., "The Flow Pattern of a Supersonic Projectile," *Communications on Pure and Applied Mathematics*, Vol. 5, No. 3, Aug. 1952, pp. 301–348.
[10] Plotkin, K. J., "Review of Sonic Boom Theory," AIAA Paper 89-1105, April 1989.
[11] Sullivan, B. M., "Human Response to Simulated Low-Intensity Sonic Booms," *NoiseCon04*, Baltimore, MD, July 2004, http://techreports.larc.nasa.gov/ltrs/PDF/2004/mtg/NASA-2004-noisecon-bms.pdf.
[12] Stevens, S. S., "Perceived Level of Noise by Mark VII and Decibels (E)," *Journal of the Acoustical Society of America*, Vol. 51, No. 2, Pt. 2, Feb. 1972, pp. 575–601.